

Arabidopsis thaliana VTC4 Encodes L-Galactose-1-P Phosphatase, a Plant Ascorbic Acid Biosynthetic Enzyme*

Received for publication, February 14, 2006, and in revised form, March 28, 2006. Published, JBC Papers in Press, April 4, 2006, DOI 10.1074/jbc.M601409200

Patricia L. Conklin^{†1}, Stephan Gatzek^{‡2}, Glen L. Wheeler^{§3}, John Dowdle[§], Marjorie J. Raymond[§], Susanne Rolinski[§], Mikhail Isupov[§], Jennifer A. Littlechild[§], and Nicholas Smirnov^{§4}

From the [†]Department of Biological Sciences, State University of New York, Cortland, New York 13045 and [§]School of Biosciences, University of Exeter, Exeter EX4 4QD, United Kingdom

In plants, a proposed ascorbate (vitamin C) biosynthesis pathway occurs via GDP-D-mannose (GDP-D-Man), GDP-L-galactose (GDP-L-Gal), and L-galactose. However, the steps involved in the synthesis of L-Gal from GDP-L-Gal *in planta* are not fully characterized. Here we present evidence for an *in vivo* role for L-Gal-1-P phosphatase in plant ascorbate biosynthesis. We have characterized a low ascorbate mutant (*vtc4-1*) of *Arabidopsis thaliana*, which exhibits decreased ascorbate biosynthesis. Genetic mapping and sequencing of the *VTC4* locus identified a mutation (P92L) in a gene with predicted L-Gal-1-P phosphatase activity (At3g02870). Pro-92 is within a β -bulge that is conserved in related *myo*-inositol monophosphatases. The mutation is predicted to disrupt the positioning of catalytic amino acid residues within the active site. Accordingly, L-Gal-1-P phosphatase activity in *vtc4-1* was ~50% of wild-type plants. In addition, *vtc4-1* plants incorporate significantly more radiolabel from [2-³H]Man into L-galactosyl residues suggesting that the mutation increases the availability of GDP-L-Gal for polysaccharide synthesis. Finally, a homozygous T-DNA insertion line, which lacks a functional At3g02870 gene product, is also ascorbate-deficient (50% of wild type) and deficient in L-Gal-1-P phosphatase activity. Genetic complementation tests revealed that the insertion mutant and *VTC4-1* are alleles of the same genetic locus. The significantly lower ascorbate and perturbed L-Gal metabolism in *vtc4-1* and the T-DNA insertion mutant indicate that L-Gal-1-P phosphatase plays a role in plant ascorbate biosynthesis. The presence of ascorbate in the T-DNA insertion mutant suggests there is a bypass to this enzyme or that other pathways also contribute to ascorbate biosynthesis.

L-Ascorbic acid (vitamin C) has been the subject of much research from the time it was first identified as the anti-scorbutic factor (1, 2). It is used as a cofactor by a number of enzymes (3), but it is perhaps better known for its role as an antioxidant. Many different organisms make use

of ascorbate to detoxify the variety of reactive oxygen species (ROS⁵; ¹O₂, O₂⁻, H₂O₂, and HO[•]) that are generated as a result of an aerobic life-style. One electron can be donated from ascorbate, forming monodehydroascorbate (ascorbate-free radical), whereas donation of a second electron results in production of the fully oxidized dehydroascorbate (4). Both plants and animals possess monodehydroascorbate and dehydroascorbate reductases to recycle the oxidized forms back to ascorbate (5).

Ascorbate is highly abundant in plant tissues, with concentrations in the 1–20 mM range, and not surprisingly has a major function in the maintenance of ROS homeostasis. ROS are formed as by-products of a variety of physiological processes, including the β -oxidation of fatty acids, photosynthesis, and photorespiration. The role of ascorbate in the detoxification of ROS generated by both abiotic and biotic environmental conditions (e.g. chilling, high light, drought, NaCl, heat, heavy metals, air pollutants, and pathogens) has been well studied for a number of years and is the subject of several recent reviews (6). Inherent within the role of ascorbate in the maintenance of ROS homeostasis is its probable role in ROS-mediated signaling (7, 8). In short, ascorbate contributes largely to both the removal of excess damaging ROS and the control of physiologically active levels of ROS utilized in signaling networks.

Ascorbate-deficient *Arabidopsis thaliana* mutants representing four different loci have been described that are valuable tools in the understanding of the physiological roles of ascorbate. The first of these mutants, *vtc1-1* (vitamin c 1), was isolated in a screen for ozone-sensitive mutants (7) and contains ~25–30% of the wild-type (WT) level of ascorbate. In addition to its sensitivity to ozone, this mutant has enhanced sensitivity to sulfur dioxide and ultraviolet B radiation (7), increased genome instability (9), and constitutively induced defense proteins that correlate with increased levels of salicylic acid and resistance to virulent strains of both *Pseudomonas syringae* and *Peronospora parasitica* (6). The *vtc1-1* mutant has altered expression of 171 transcripts, including those of several defense genes and genes involved in hormone signaling (10). It also exhibits signs of premature senescence, both visually and at the molecular level, which has led to the idea that the pathogen resistance of this mutant may be age-related (6). The second ascorbate-deficient complementation group, *vtc2*, was isolated in a nitro blue tetrazolium-based screen (11). The mutant *vtc2-2* has been utilized to better understand the role of ascorbate in both violaxanthin de-epoxidase activity *in vivo* (12) and in acclimation of photosynthesis to high light (13). The *VTC2* gene has been cloned but its function is as yet unknown (14). The ascorbate-deficient mutants *vtc3-1* and *vtc4-1* were also isolated in the above-mentioned nitro blue tetrazolium-based

* The costs of publication of this article were defrayed in part by the payment of page charges. This article must therefore be hereby marked "advertisement" in accordance with 18 U.S.C. Section 1734 solely to indicate this fact.

¹ Supported by the National Research Initiative of the United States Department of Agriculture Cooperative State Research, Education, and Extension Service Grant 1998-35100-12987 and a grant from the Dr. Nula McGann Drescher Affirmative Action/Diversity Leave Program.

² Present address: Novartis Pharma AG, Biomarker Development, WKL-136.1.15, CH-4002 Basel, Switzerland.

³ Present address: Plymouth Marine Laboratory, Prospect Place, The Hoe, Plymouth PL1 3DH, UK.

⁴ Supported by the Biotechnology and Biological Sciences Research Council (UK) and Bio-Technical Resources (Manitowoc, WI). To whom correspondence should be addressed: School of Biosciences, Geoffrey Pope Bldg., University of Exeter, Stocker Road, Exeter EX4 4QD, UK. Tel.: 44-1392-263756; Fax: 44-1392-263700; E-mail: N.Smirnov@exeter.ac.uk.

⁵ The abbreviations used are: ROS, reactive oxygen species; BC2, backcross 2; DTT, dithiothreitol; Fru, fructose; Fuc, fucose; Gal, galactose; Glc, glucose; Gul, gulose; IMPase, inositol monophosphatase; Man, mannose; WT, wild type; HPLC, high pressure liquid chromatography; KO, knock out; RT, reverse transcription; F, forward; R, reverse; PAP, 3'-phosphoadenosine 5'-phosphate.

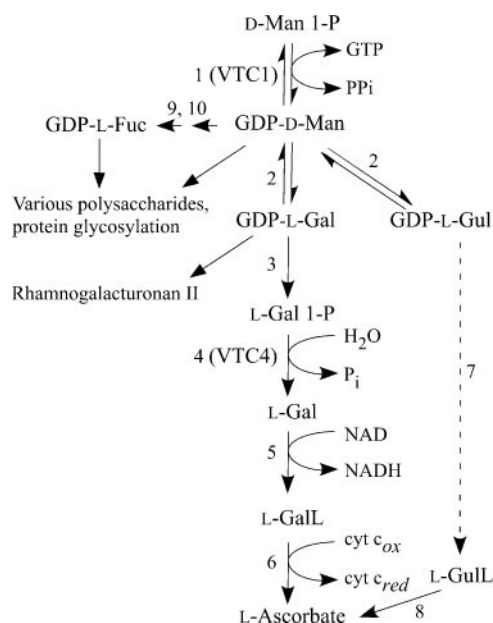


FIGURE 1. The D-Man/L-Gal pathway for L-ascorbic acid biosynthesis in plants (15). In this pathway, the carbon skeleton from D-Man-1-P (synthesized from D-Glc-1-P via D-Fru-6-P) is converted through a series of intermediates, including L-Gal and L-galactono-1,4-lactone to L-ascorbic acid. Enzymes that catalyze the conversions are as follows: step 1, GDP-D-Man pyrophosphorylase (*A. thaliana* VTC1/At2g39770; see Ref. 17); step 2, GDP-D-Man-3,5-epimerase (19, 21); step 3, GDP-L-Gal breakdown enzyme; and step 4, L-Gal-1-P phosphatase (*A. thaliana* VTC4/At3g02870; see Ref. 23). Its function in ascorbate synthesis as described in this paper is as follows: step 5, L-Gal dehydrogenase (18); step 6, L-galactono-1,4-lactone (L-GalL) dehydrogenase (located in mitochondrial electron transport complex I; see Ref. 52); step 7, these steps are not characterized but could utilize enzymes 3–5; and step 8, L-gulonolactone oxidase/dehydrogenase. Activity exists in plants but is not fully characterized (21, 53); step 9, GDP-D-mannose-4,6-dehydratase (*A. thaliana* MUR1; see Ref. 42); step 10, GDP-4-keto-6-deoxy-D-mannose 3,5-epimerase-4-reductase (*A. thaliana* GER1; see Ref. 39).

screen and at 2 weeks of age were found to contain less than 50% of WT levels of ascorbate (11).

In addition to the utility of *vtc1-1* mutant as an aid in the functional analysis of ascorbate, it has also proven invaluable as a genetic tool in the study of ascorbic acid biosynthesis in plants. In 1998, a novel plant ascorbic acid biosynthetic pathway was proposed in which L-Gal is oxidized sequentially to L-galactono-1,4-lactone and ascorbate (15, 16) (Fig. 1). The newly proposed pathway resolved a puzzle regarding the source of substrate for the previously well characterized plant L-galactono-1,4-lactone dehydrogenase (15). Radiolabeling studies showed that L-Gal is derived from GDP-Man (15). Functional *in planta* evidence for this pathway was provided by the *VTC1* gene, which encodes GDP-Man pyrophosphorylase and forms GDP-Man from Man-1-P (Fig. 1) (17). The *vtc1-1* mutant has a point mutation in this gene, lowered activity of this enzyme, and is ascorbate-deficient. In addition to the GDP-Man pyrophosphorylase gene, the genes encoding GDP-Man 3",5"-epimerase, L-galactono-1,4-lactone dehydrogenase, and the L-Gal dehydrogenase have also been identified (18–20). GDP-Man 3",5"-epimerase converts GDP-Man to GDP-L-Gal, which is then proposed to be broken down in two steps to L-Gal (Fig. 1, steps 3 and 4). Additionally, it has been shown that GDP-L-gulose is also produced as a result of GDP-Man 3",5"-epimerase activity and could be converted to ascorbate via L-gulonolactone (Fig. 1) (21). Reduction of L-Gal dehydrogenase and L-galactono-1,4-lactone dehydrogenase activities *in planta* (via antisense suppression) leads to reduced levels of ascorbate (18, 22). Recently, a gene encoding an enzyme with L-Gal-1-P phosphatase activity was identified in kiwi fruit and *A. thaliana* (23). This enzyme is predicted to take part in ascorbate biosynthesis (Fig. 1, step 4). As described below, we have found that the ascorbate-deficient *A. thaliana*

vtc4-1 mutant harbors a defect in the same L-Gal-1-P phosphatase gene, providing genetic evidence for the role of this enzyme in plant ascorbate biosynthesis.

EXPERIMENTAL PROCEDURES

Measurement of Ascorbate Content—Acidic extracts were prepared from whole rosettes of 3-week-old *vtc4-1* (backcross 2 generation; BC2) and WT ecotype Columbia-0 for the assay of the total and reduced ascorbate as described previously (7, 24). At least three whole rosettes were used in each extract, and the average ascorbate (total and reduced) content from five extracts/genotype was determined. The plants used for these assays were grown with a 16-h photoperiod under metal halide bulbs in a commercial soil-less mix (Promix BX; Premier Horticulture Inc., Quakertown, PA). For the assay of total ascorbate in WT, *vtc4-1* BC2, insertion line KO-1, insertion line KO-2, F₁ (*vtc4-1* × KO-1), F₁ (*vtc4-1* × KO-2), expanded leaves from at least three different 2-week-old rosettes were utilized for each extract, and the average total ascorbate was determined from three extracts/genotype. The plants used for these assays were grown in an environmental growth chamber (Percival AR36L3) under a 24-h photoperiod at 21 °C with 70% relative humidity under fluorescent bulbs at 150 μmol s⁻¹ m⁻² photosynthetic photon flux density.

Fine-scale Genetic Mapping of the VTC4 Locus—The *VTC4* locus was found to be located ~2-centimorgan centromeres distal from microsatellite marker nga172 as described previously (11). A population of 1772 F₂ individuals derived from a cross between *VTC4/VTC4* (*Landsberg erecta* ecotype) and *vtc4-1/vtc4-1* (Columbia-0 ecotype) was utilized in the fine-scale genetic mapping. The *VTC4*-specific genotype of each recombinant was verified in the F₃ generation. The insertion/deletion marker (12/–12; CER469590; Cereon *Arabidopsis* Polymorphism Collection, see Ref. 14) that defined the closest centromere distal breakpoint was amplified using the following primers: 5'-ACAACAATGGC-GATCA-3' and 5'-CATCCTCTGGTAAAGACAC-3'. This marker is located at ~70 kb on BAC F13E7. The three tightly linked single nucleotide polymorphism markers that defined the closest centromere proximal recombination breakpoint (CER467138-140; Cereon *Arabidopsis* Polymorphism Collection, see Ref. 14) were amplified and sequenced using the following primers: 5'-ACGCGACAGCTTCCATT-3' and 5'-GGCTTGCGTGAGTGTATTCTTTCT-3'. These tightly linked single nucleotide polymorphisms are located at ~26 kb on BAC F13E7. All amplifications in this study were performed using a PCRExpress thermocycler (ThermoElectron Corp., Waltham, MA) unless stated otherwise.

Sequencing of the VTC4 Locus—Total DNA was isolated from *vtc4-1* (BC2) and Columbia-0 WT using a cetyltrimethylammonium bromide mini-prep method as described previously (25). The *VTC4* locus was amplified from these DNAs using two PCR primer pairs (Sigma Genosys, The Woodlands, TX) that together amplified the *VTC4* candidate gene (At3g02870). One set of primers (F, 5'-CGTTGGGACTGGC-TGTATC-3'; R, 5'-AAACAACCTCCAACAACAGGG-3') amplified a 2036-bp product, including 1193 bp upstream of the ATG start codon. A second set of primers (F, 5'-CCAATTCGTTACACGGGTAT-3'; R, 5'-GGACAACAGTCACCGTGAGA-3') amplified a 1749-bp overlapping product that included 488 bp 3' of the stop codon. Sequencing primers nested within these two products (and in some cases, single PCR primers) were used to obtain genomic sequence from *vtc4-1* that spanned from 715 bases upstream of the putative 5'-transcript terminus to 192 bp downstream of the putative 3'-transcript terminus (Biotechnology Resource Center, Cornell University, Ithaca, NY). Both strands of *vtc4-1* DNA were sequenced in the region of the mutation. One

Ascorbate Synthesis in Plants via L-Gal-1-P Phosphatase

strand of WT Columbia-0 DNA was sequenced in this same region to verify the published WT genomic sequence.

Identification of Homozygous Insertion Mutant at the VTC4 Locus—Segregating T3 generation seed for the SAIL_8443_G10 sequence indexed insertion line (26) was obtained from the Arabidopsis Biological Resource Center. Total DNA was isolated from 16 individual plants as described above. The VTC4 locus was amplified from these DNAs using the second set of (flanking) primers described above. Those individual lines that did not yield a PCR product with these VTC4 WT allele-specific primers were then each amplified in a series of two separate PCRs using the insertion primer LB1 (5'-GCCCTTTCAGAAATGGATAAATAGCC TTGCTTCC-3') and either the F or R flanking primers. Five homozygous insertion individuals and six heterozygous individuals were identified using this series of amplification reactions. To confirm the site of the insertion, the ~1.5-kb PCR product obtained from amplification of line 11 with LB1 and the VTC4 R flanking primer was gel-purified and sequenced as above using the LB1 insertion-specific primer as the sequencing primer.

To confirm the genotypes of the F₁ (*vtc4-1* × KO-1) and F₁ (*vtc4-1* × KO-2) individuals, DNA was extracted from at least five F₁ plants derived from each cross as described above and genotyped by PCR in two separate reactions/genotype (along with WT, *vtc4-1*, KO-1 T4, and KO-2 T4 DNAs as controls) using the VTC4 flanking F and R primers in one reaction (noninsertion allele specific product) and the VTC4 R and LB1 primers in a second reaction (insertion allele-specific product).

RNA Extraction and RT-PCR—For the semi-quantitative assay of transcript levels in *vtc4-1* in comparison with WT, the following protocol was utilized. Total RNA was isolated from *Arabidopsis* leaves collected just prior to flowering using an RNeasy plant RNA kit (Qiagen, Crawley, UK) and treated with DNase (Qiagen, Crawley, UK) according to the manufacturer's instructions. Synthesis of cDNA was carried out, using 5 μg of total RNA as template, with random primers (RETROscript, Ambion, Huntingdon, UK) and Superscript II (Invitrogen). Semi-quantitative PCR, using the cDNA as template, was performed using an 18S Competimer system (Ambion, Huntingdon, UK) according to the manufacturer's instructions. Primers used in the PCR were 5'-GGAAAGGAGCATTCTTGAATGG-3' and 5'-CAACGCCTCAGC-GAATAAC-3' and the cycling parameters consisted of 2 cycles (96 °C 1 min, 50 °C 30 s, and 72 °C 1 min) followed by 32 cycles (92 °C 25 s, 54 °C 30 s, and 72 °C 1 min) and a 10-min extension at 72 °C.

For the assay of the presence/absence of transcript in WT, *versus* the insertion lines KO-1 and KO-2, total RNA was isolated from 100 mg of *Arabidopsis* leaves collected from plants 20 days of age that were grown in an environmental growth chamber (Percival AR36L3) under the same conditions as the plants utilized for the total ascorbate assays described above. The RNA was isolated using the RNeasy plant mini kit (Qiagen, Crawley, UK). Synthesis of cDNA was carried out using 1 μg of total RNA as the template, with the VTC4RTR 5'-CAACGCCTCAGC-GAATAAC-3', the UBQ10R 5'-CGACTTGTTCATTAGAAAAGAAAGAGATAACAGC-3', and ferredoxin-nitrite reductase R 5'-CCACG-GATCTGCCAATTCTGT-3' gene-specific primers and Moloney murine leukemia virus RT (Promega Corp., Madison, WI). Nonquantitative PCRs were then performed using the above cDNAs as templates and the following primers in addition to the reverse primers listed above: VTC4RTF 5'-GGAAAGGAGCATTCTTGAATGG-3, UBQ10F 5', UBQF 5'-GATCTTTGCCGAAAACAATTGGAGGATGG-3', and ferredoxin-nitrite reductase F 5'-TCCGGTTCCACCTGCCAACA-3'. Cycling parameters consisted of 1 cycle (95 °C 3 min) followed by 40 cycles (94 °C 20 s, 54 °C (VTC4RTF/R and ferredoxin-nitrate reductase F/R) or 58 °C (UBQFR) 20 s, 72 °C 1 min) and a 5-min extension at 72 °C.

Ascorbate Biosynthesis from [U-¹⁴C]Man and [1-¹⁴C]Ascorbate Metabolism—D-[U-¹⁴C]Man (1 μCi per sample, specific activity 290 mCi mmol⁻¹; Amersham Biosciences) or [1-¹⁴C]ascorbate (27) was supplied via the petiole to whole excised *Arabidopsis* leaves from 6-week-old plants. Following radiolabel uptake (1 h), leaves were illuminated (60–70 μmol m⁻² s⁻¹ photosynthetic photon flux density) in sealed Perspex boxes for 4 h. Leaves were rinsed thoroughly prior to perchloric acid extraction and determination of incorporation of [¹⁴C]ascorbate and other fractions as described previously (24). Briefly, leaf tissue was ground in liquid nitrogen, homogenized in 1 ml of 5% perchloric acid, 1 mM EDTA, and centrifuged (12,000 × g, 2 min, 4 °C). The supernatant was neutralized by the addition of 60 μl of 5 M potassium carbonate and centrifuged again (12,000 × g, 2 min, 4 °C). The ascorbate concentration in the resultant supernatant was determined by the ascorbate oxidase method (24), prior to ion exchange fractionation. This allowed determination of the recovery of ascorbate after ion exchange and HPLC separation. The resultant supernatant was mixed with an equal volume of 10% dithiothreitol (DTT) and fractionated by ion exchange chromatography (SAX column, HPLC Technology, Macclesfield, UK). Ascorbate was eluted from the column with 60 mM formic acid. The eluent was immediately frozen in liquid nitrogen and lyophilized. Samples were reconstituted in 6 mM formic acid and loaded onto a Rezex ROA HPLC column (Phenomenex, Macclesfield, UK) using a mobile phase of 0.75 mM sulfuric acid (0.5 ml min⁻¹). Ascorbate was detected by UV absorbance at 260 nm. The identity of the ascorbate peak was confirmed in preliminary experiments by treatment of the samples with ascorbate oxidase. This removed the peak detected by HPLC at 260 and 210 nm. Radioactivity in the eluent fractions corresponding to ascorbate was determined by liquid scintillation counting. The rate of turnover of ascorbate was calculated from [1-¹⁴C]ascorbate metabolism as described previously (27).

Incorporation of D-[2-³H]Man into Polysaccharides—D-[2-³H]Man (2–5 μCi, specific activity 10–20 Ci/mmol) (Amersham Biosciences) was supplied to small expanding leaves from young *Arabidopsis* plants (2–3 weeks old) via their petioles. Following uptake of the radiolabel (2 h), leaves were illuminated (60–70 μmol m⁻² s⁻¹ photosynthetic photon flux density) in sealed Perspex boxes for 4 h. Samples were then rinsed thoroughly prior to homogenization in ice-cold 80% ethanol. Insoluble material was collected by centrifugation (12,000 × g, 2 min) and washed three times with 80% ethanol. Polysaccharides and oligosaccharides associated with glycoproteins in this material were hydrolyzed by incubation with 2 M trifluoroacetic acid at 110 °C for 1 h (28). Nonhydrolyzed material was removed by centrifugation (12,000 × g, 2 min), and trifluoroacetic acid was removed from the supernatant by evaporation. Monosaccharides were separated by TLC (29). Separation was performed by an acetone/butanol/water solvent (8:1:1 v/v) on silica gel TLC plates (Whatman) pre-soaked in 0.3 M sodium dihydrogen orthophosphate and then dried. The radioactivity was detected by a Berthold LB2832 Linear Analyser (Wildbad, Germany). Radioactive peaks were identified by co-chromatography with authentic standards. D-Gal was removed by treatment with D-Gal dehydrogenase (from *Pseudomonas fluorescens*, Sigma). The reaction mixture contained 0.1 unit of D-Gal dehydrogenase and a 10-μl sample in 175 μl of 50 mM Tris-HCl, pH 8.6, containing 7 mM NAD⁺ and was incubated for 16 h. Samples were then deionized by ion exchange chromatography to facilitate TLC analysis. This technique fully resolves L-Fuc, L-Gal, and D-Man, but L-Gul is not resolved from D-Man.

Assay of L-Gal-1-P Phosphatase—Rosette leaves from plants just prior to flowering, grown under a 16-h light period at 150 mmol s⁻¹ m⁻² photosynthetic photon flux density (20 °C during light period, 15 °C

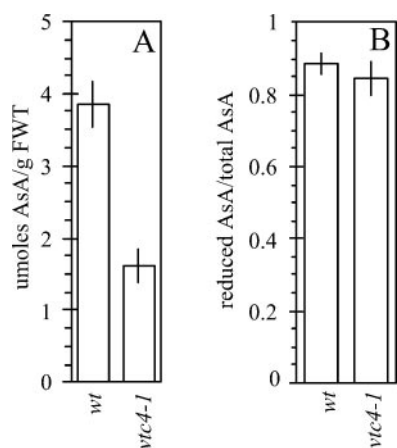


FIGURE 2. The *Arabidopsis* mutant *vtc4-1* is deficient in total ascorbate, whereas the redox status of ascorbate in this mutant is unaffected. *A*, total ascorbate concentration in 3-week-old WT and *vtc4-1* plants. The values represent the means of five replicate assays (error bars represent the S.D.), and each replicate sample included rosettes from at least three individuals. *B*, the ratio of reduced to total ascorbate in 3-week-old WT and *vtc4-1* plants. Reduced ascorbate in each of the above-mentioned samples was assayed by the ascorbate oxidase assay with the omission of DTT. Oxidized ascorbate was obtained by subtraction.

during dark period), were homogenized in 50 mM Hepes, pH 7.5, 10 mM MgCl₂, 2 mM DTT, 1 mM aminocaproic acid, 1 mM benzamidine, 1 mM phenylmethylsulfonyl fluoride (5 g of tissue, 10 ml of extract). Duplicate extracts were made for each experiment, and the experiments were repeated on two occasions with identical results. Tissue debris was filtered off, and the homogenate was centrifuged at 20,000 × *g* for 20 min at 4 °C. Ammonium sulfate was added to the supernatant to 40% saturation, and precipitated protein was pelleted by centrifugation as before for 30 min. The supernatant was collected and ammonium sulfate added to give 60% saturation. After centrifugation, the pelleted protein was recovered. This was dissolved in 25 mM Tris-HCl, pH 7.5, containing 1 mM DTT. L-Gal-1-P phosphatase activity was determined by incubating a 10-μl sample with 80 μl of 50 mM Tris-HCl, pH 7.5, containing 0.1 mM L-Gal-1-P and 3 mM MgCl₂ for 1 h. The reaction mixture was then boiled for 2 min and centrifuged at 12,000 × *g* for 2 min. L-Fucose (L-Fuc; 0.05 mM final concentration) was added as an internal standard. The sugars in 20 μl of this sample were separated and quantified using a Dionex DX600 LC with a CarboPac PA-10 column and electrochemical detection. The mobile phase was 18 mM NaOH at 1 ml min⁻¹, and the column was washed with 200 mM NaOH between samples. The ED₅₀ electrochemical detector was equipped with a gold electrode and was operated in pulsed amperometric mode specific for sugars (waveform: 0 s at -0.05 V, 0.2 s at 0.05 V (integration on) 0.4 s at 0.05 V (integration off) 0.41 s at 0.075 V, 0.6 s at 0.75 V, 0.61 s at -0.15 V, 1.00 s at -0.15 V). The L-Gal-1-P was a gift from J. Thiem (University of Hamburg, Germany).

RESULTS

Decreased Ascorbate Synthesis from Man in *vtc4*—As described previously (11), the *A. thaliana* mutant *vtc4-1* (vitamin C 4) was isolated in a nitro blue tetrazolium-based screen for ascorbic acid-deficient ethane methyl sulfonate-generated mutants of the Columbia-0 ecotype. *VTC4* is one of four *VTC* loci identified by this screen (6). At 3 weeks of age, the homozygous *vtc4-1* mutant contains ~42% of the total ascorbate found in WT plants (Fig. 2A). Although deficient in total ascorbate, the redox status of *vtc4-1* (the ratio of total to reduced ascorbate) does not significantly differ from that of WT (Fig. 2B). Both genotypes maintain a highly reduced pool of ascorbate (~88% for WT and ~85% for *vtc4-1*). Radiolabeling experiments were carried out to determine whether the

TABLE 1
Ascorbic acid biosynthesis from D-[U-¹⁴C]mannose in the *vtc4-1* mutant

The distribution of radioactivity in whole *Arabidopsis* leaves supplied D-[U-¹⁴C]mannose via the petiole for 1 h in the light. Leaves were enclosed in Perspex boxes and incubated for a further 4 h in the light prior to extraction and fractionation. Radioactivity in ascorbic acid was measured after ion exchange chromatography and HPLC separation of the soluble fraction and was adjusted for recovery. Standard errors are shown (*n* = 3).

Fraction	Wild type	<i>vtc4-1</i>
	% total	
Ethanol-insoluble	19.7 ± 0.7	18.0 ± 4.4
Soluble	78.3 ± 0.9	77.8 ± 4.8
CO ₂	2.0 ± 0.2	4.1 ± 0.7
Ascorbic acid	19.0 ± 2.0	13.5 ± 2.0

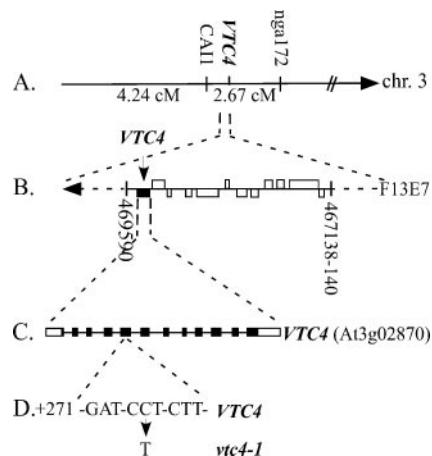


FIGURE 3. Fine-scale genetic mapping narrowed the site of the *VTC4* locus and sequencing of the candidate L-Gal-1-P phosphorylase gene and led to the identification of a point mutation in the ascorbate-deficient *vtc4-1* mutant. *A*, using a polymorphic F₂ mapping population (from *VTC4/VTC4* in Ler ecotype × *vtc4-1/vtc4-1* in Col-0 ecotype), the *VTC4* locus was genetically mapped near the top of chromosome 3 to a region ~2-centimorgan centromeres distal from the microsatellite marker nga172 (11). The arrow represents the locale of the centromere relative to this region. *B*, fine-scale mapping with the use of 1772 F₂ individuals narrowed the *VTC4* locus to a genomic region residing on BAC F13E7 between the single nucleotide polymorphisms CER469590 and CER467138-140. This region contained 12 candidate genes as annotated by the Arabidopsis Genome Project. These candidate genes are represented by rectangles. *C*, the structure of candidate gene At3g02870, an enzyme with *in vitro* L-Gal-1-P phosphorylase activity, is shown. Filled rectangles represent exons, and open rectangles represent the 5'- and 3'-untranslated regions. *D*, the cytosine at nucleotide +275 relative to the initiation ATG of At3g02870 in WT and the thymidine transition mutation in the ethane methyl sulfonate-generated *vtc4-1* mutant.

low ascorbate content of *vtc4* is caused by slower biosynthesis via the D-Man pathway or by faster catabolism. Leaves were labeled with D-[¹⁴C]Man, extracted, and fractionated into soluble and insoluble compounds and CO₂. Ascorbate was separated by HPLC and its ¹⁴C content determined. 30% less ¹⁴C was incorporated into ascorbate in *vtc4-1* compared with WT, whereas the distribution of label in other fractions did not differ (Table 1). This compares closely to the 42% reduction in ascorbate content. Feeding [¹⁴C]ascorbate and determining the transfer of ¹⁴C to other compounds estimated ascorbate turnover (27). The turnover of ascorbate in *vtc4-1* under these conditions was 0.63 ± 0.06 μmol 5 h⁻¹ g⁻¹ fresh weight, compared with 0.72 ± 0.1 μmol 5 h⁻¹ g⁻¹ fresh weight in wild type. These results suggest that low ascorbate in *vtc4-1* is caused by a slower rate of biosynthesis from D-Man.

Genetic Evidence That *VTC4* Encodes L-Gal-1-P Phosphatase and That This Enzyme Is Involved in Ascorbate Biosynthesis—The *VTC4* locus was initially mapped to the top of chromosome III, ~2-centimorgan centromeres distal from the microsatellite marker nga172 (Fig. 3A) (11), which is located at 6.91 centimorgans. By using a mapping population of 1772 F₂ individuals derived from a cross between *vtc4-1* and the

Ascorbate Synthesis in Plants via L-Gal-1-P Phosphatase

```

75 EPTWIIIDPLDGTTNFV consensus
84 nPTWIIIDPIdGTTNFV B. taurus
83 nPTWIIIDPIDGTTNFV H. sapiens
87 nPTWIIIDPIDGTTNFV X. laevis
88 gPTfIVDPIDGTTNFV S. cerevisiae
149 aPTWIIIDPIDGTTNFV C. elegans
78 dvqWVIDPLDGTTNFV E. coli
90 pfcWaIDPLDGTTNFa Synechocystis
159 dylWcIDPLDGTTNFa A. thaliana At1g31190
85 EPTWIVDPLDGTTNFV A. thaliana At3g02870

85 EPTWIVDLLDGTTNFV vtc4-1

```

FIGURE 4. Alignment of the region containing a highly conserved domain (enclosed by rectangle) of selected IMPase polypeptides within the IMPase family (HomoloGene). Amino acid residues in capital letters are those shared with the consensus. Amino acids whose side chains were recently shown to be ligands for Mg^{2+} binding in the active site of the *Bos taurus* IMPase (33) are underlined. The conserved proline residue (Pro-92) whose codon is mutated to encode a leucine in *vtc4* is in boldface type. *B. taurus*, P20456; *Homo sapiens*, 2HHM_A; *Xenopus laevis*, P29219; *Saccharomyces cerevisiae*, AAB64472; *Caenorhabditis elegans*, Q19420; *E. coli*, P22783; *Synechocystis*, P74158; *A. thaliana* At1g31190, NP_564376; and *A. thaliana* At3g02870, NP_186936.

wild-type Ler ecotype, the *VTC4* locus was narrowed genetically to the region between insertion/deletion CER469590 (70,345–70,358 bp) on BAC F13E7 and single nucleotide polymorphism CER467138-140 (26,032–26,203 bp) on the ~100-kb BAC F13E7 (Fig. 3B). The centromere distal recombination breakpoint was defined by two recombinants, whereas the centromere proximal breakpoint was defined by three recombinants. This region spans ~44 kb and contains 12 candidate genes (Fig. 3C).

One of the 12 candidate *VTC4* genes (At3g02870) has been annotated as encoding a *myo*-inositol monophosphatase-like protein (TAIR; see Ref. 30). However, Laing *et al.* (23) recently published evidence demonstrating that this gene (and its homologue in kiwi fruit) encodes an enzyme with L-Gal-1-P phosphatase activity *in vitro* and upon expression in *Escherichia coli*. As L-Gal-1-P phosphatase is predicted to play a role in the D-Man/L-Gal ascorbic acid biosynthetic pathway (15, 23) catalyzing the conversion of L-Gal-1-P to L-Gal (Fig. 1), we sequenced At3g02870 in *vtc4-1*. Indeed, *vtc4-1* harbors a cytosine to thymine point mutation within exon 5 at nucleotide +275 relative to the first nucleotide of the predicted methionine start codon (Fig. 3D). As this mutant was generated by ethane methyl sulfonate, a C/G to T/A transition mutation was not unexpected. The transcript abundance of the L-Gal-1-P phosphatase mRNA in *vtc4-1* and WT leaves, just prior to flowering, was determined with RT-PCR. The abundance of L-Gal-1-P phosphatase-specific mRNA is quite low in both genotypes but is not significantly lower in the mutant (data not shown).

The predicted *VTC4* (At3g02870) gene product belongs to a group of polypeptides with a conserved domain defined by the HomoloGene system of the NCBI (cd01639). This conserved domain group includes primarily members of the inositol monophosphatase (IMPase) family of genes. IMPases function as homodimers. Many of these members utilize inositol monophosphate as a substrate, but some have phosphatase activity toward other substrates such as fructose 1,6-bisphosphate (31). The cd01639 group all encode either predicted or experimentally confirmed Mg^{2+} -dependent phosphatases that are inhibited by lithium. The L-Gal-1-P phosphatase activity encoded by *Actinidia deliciosa*, and the *Arabidopsis* enzyme encoded by At3g020870, is completely dependent *in vitro* on Mg^{2+} for activity, and furthermore, the *A. deliciosa* enzyme is inhibited strongly by lithium (23). A highly conserved domain shared by this group is composed of six amino acids. An amino acid alignment of the region containing this domain in representatives from cd01639 is shown (Fig. 4). The *VTC4* protein structure has been modeled using the Swiss model homology model server (32) using the

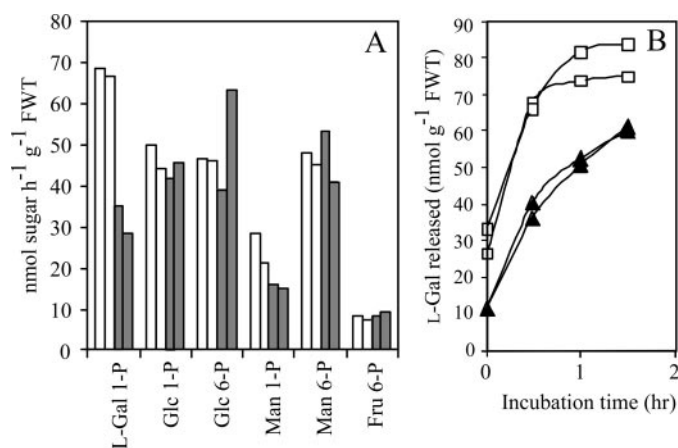


FIGURE 5. L-Gal-1-phosphate phosphatase activity is reduced in the *vtc4-1* mutant. Leaf extracts from plants just prior to flowering were fractionated by ammonium sulfate precipitation (45–60% saturation). The desalted sample was incubated with various sugar phosphates. Released sugars were measured by LC-pulsed amperometric detection. A, comparison of phosphatase activity toward various sugar phosphates by WT (open bars) and *vtc4-1* (shaded bars) extracts. B, time course of L-Gal-1-P hydrolysis by WT (open squares) and *vtc4-1* (filled triangles) extracts.

known three-dimensional structures of several inositol phosphatase enzymes, with which *VTC4* shares 40–41% sequence identity (33–35). The resulting model was compared with the structure of human inositol phosphatase containing the substrate *D*-*myo*-inositol 1-phosphate (36) (Protein Data Bank code 1IMB). Most structural features of substrate- and metal-binding sites are conserved between the x-ray structure and the *VTC4* model. The residue Pro-92 is located on a stretch of about 30 residues with high sequence conservation that spans through β -strands β D and β E and includes helix α 3. The Pro-92 is involved in formation of a β -bulge of the so-called “wide class” (37) at the C terminus of strand β D. This structural feature allows the positioning of the side chains of Asp-91 and Asp-94 and main chain oxygen of Ile-93 to coordinate magnesium ions required for the catalytic activity and side chain of Asp-94 in the vicinity of the scissile phosphoester bond. Such β -bulges are usually structurally conserved throughout a protein family. The P92L mutation in *VTC4* will cause unfavorable steric clashes with residues from the neighboring strand β C and helix α 2, which are likely to cause the distortion of the β -bulge. Provided the P92L mutant protein folds correctly, the likely consequences of the mutation will be the displacement of side chains of Asp-91 and Asp-94, which coordinate the metal ions and are postulated to be important for the expulsion of the ester oxygen (36). In addition, the side chain of Glu-71, which is postulated to be activating the nucleophilic water (36), is likely to be displaced because of the steric clash of strand β C with the side chain of Leu-92. Disruption of the β -bulge is likely to affect residues Gly-95 and Thr-96 of helix α 3, which are involved in the binding of the substrate phosphate group. To summarize, the mutation of P92L in *VTC4* is likely to affect positioning of several key residues important for metal and substrate binding and for catalytic activity within the enzyme active site. These changes are therefore expected to significantly reduce the catalytic activity of the *VTC4* enzyme.

To confirm the predicted effect of the mutation on L-Gal-1-P phosphatase activity, phosphatase activity was measured in the 45–65% saturation ammonium sulfate fraction of WT and *vtc4-1* leaf extracts. This fraction is enriched in L-Gal-1-P phosphatase activity assayed at pH 7.5 (see below). In each of two replicate assays, the phosphatase activity with the substrate L-Gal-1-P was reduced ~2-fold in *vtc4-1* (Fig. 5A). The specificity of this difference was confirmed by comparing the phosphatase activity toward a variety of sugar phosphates. There was no

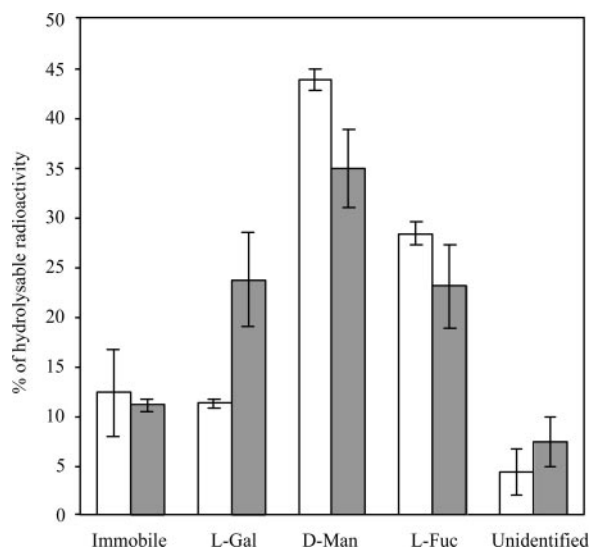


FIGURE 6. Increased incorporation of radioactivity from D-[2-³H]Man into polysaccharide L-galactosyl residues in *vtc4-1*. Whole detached leaves of WT (open bars) and *vtc4-1* (shaded bars) were supplied with D-[2-³H]Man via the petiole for a total incubation time of 6 h. Monosaccharides released by trifluoroacetic acid hydrolysis of the ethanol-insoluble leaf fraction were separated by TLC. The experiment was repeated twice with similar results, and one experiment is shown here. Ranges are S.E. ($n = 3$). The D-Man spot may also contain L-Gul as these sugars are not resolved. Immobile indicates material located on the TLC plate origin.

difference in the rate of hydrolysis of Glc-1-P, Glc-6-P, and Fru-6-P. Man-1-P was hydrolyzed more rapidly by WT extracts; however, this difference was much less marked than for L-Gal-1-P (Fig. 5B).

D-Mannose and L-Galactose Metabolism Are Affected in vtc4-1—The metabolism of mannose in *vtc4-1* and WT leaves was examined in more detail. As *vtc4-1* is impaired in L-Gal-1-P phosphatase activity, we predicted that intermediates upstream of this block in the ascorbate biosynthetic pathway might accumulate. As both GDP-D-Man and GDP-L-Gal are precursors for polysaccharides, we examined the incorporation of D-mannose into polysaccharides in WT and *vtc4-1* leaves. D-[2-³H]Man was fed to intact leaves, and the monosaccharide residues released following trifluoroacetic acid hydrolysis of the 80% ethanol-insoluble fraction (primarily cell wall) were determined by TLC. Radioactivity was detected in L-Gal, D-Man, and L-Fuc. In two independent experiments, the proportion of the radiolabel recovered in L-Gal residues from *vtc4-1* leaves was greater than the recovery from wild type. 24 and 28% of total hydrolyzable radioactivity was recovered as L-Gal from *vtc4-1*, compared with recoveries of 11 and 12% from wild-type leaves (Fig. 6). It is possible that other labeled sugars co-chromatograph with L-Gal, thus invalidating this conclusion. However, several lines of evidence suggest this possibility is unlikely. First, radiolabel appearing in L-Gal is derived directly from D-[2-³H]Man because the label is lost from C-2 if D-Man is first converted to Glc by a C-2 epimerization (38). Therefore, only sugars derived directly from D-Man could be labeled. These include L-Gul, which co-chromatographs with D-Man, and 4-keto-6-deoxy-D-mannose, which is an intermediate of GDP-L-Fuc synthesis (39) and will not occur in polysaccharides. Second, Roberts (40), using a similar chromatographic technique, demonstrated that radiolabeled L-Gal residues derived from D-Man in maize roots did not co-chromatograph with detectable quantities of any other monosaccharide after multiple recrystallizations of the L-Gal methylphenylhydrazone derivative. Third, other glycosyl residues found in plant polysaccharides (e.g. D-Glc, D-Gal, xylose, arabinose, apiose, and rhamnose) are derived from UDP-Glc (41) and will not be labeled. Any possible interfering labeled D-Gal was specifically removed by treatment with D-Gal dehydrogenase.

Phenotype of Plants Homozygous for an Insertion Mutation in the VTC4 Locus—To confirm that *VTC4* = At3g02870, we isolated and analyzed an *Arabidopsis* line homozygous for an insertion allele of At3g02870. A population of 16 individual plants of the sequence-indexed SAIL_843_G10 line segregating for a predicted insertion in At3g02870 was screened via PCR and At3g02870-specific primers to identify individuals homozygous for the insertion allele. Five such lines were identified. Two lines (KO-1 and KO-2) were used for further analysis (Fig. 7A). The site of the insertion was confirmed by sequencing to reside within exon 7; therefore, this mutant allele is predicted to be null. To determine whether the KO lines produced any *VTC4* transcript, RT-PCR was conducted using *VTC4* gene-specific primers that span exons 7 and 12. The PCR product from the *VTC4* cDNA is expected to be 382 bp. A set of control primers that span exon 1 and exon 2 of a ferredoxin-nitrite reductase gene (At2g15620) are expected to amplify a 408-bp product from the corresponding cDNA. As seen in Fig. 7B, RT-PCR using the *VTC4* gene-specific primers yielded the expected size product from WT as well as *vtc4-1* cDNAs, whereas no product of the same size was amplified from cDNAs from the insertion lines KO-1 and KO-2. There is a small amount of product in these insertion lines, but it is slightly larger than that seen in WT and *vtc4-1* and is most likely a nonspecific amplification product. The control primers yielded the expected size product from all the genotypes. Total ascorbate was determined in 2-week-old insertion mutant lines KO-1 and KO-2 along with WT and *vtc4-1*. As seen in Fig. 7C, both insertion mutant lines are deficient in ascorbate, with a deficiency quite similar to that of *vtc4-1* grown under the same conditions. Furthermore, L-Gal-1-P phosphatase activity was reduced in the two KO lines. Similarly to *vtc4-1*, the extracts also hydrolyzed Man-1-P at a slightly lower rate than WT (Fig. 7D).

To confirm genetically that the mutations that cause the ascorbate deficiencies in *vtc4-1* and the insertion lines are allelic, genetic complementation analyses were conducted. The *vtc4-1* line was used as the female to generate F₁ progeny between *vtc4-1* and KO-1 and between *vtc4-1* and KO-2. DNA was isolated from pooled F₁ individuals from each cross and the genotype confirmed by PCR. As seen in Fig. 8A, the WT and *vtc4-1* individuals harbor noninsertion alleles, and the KO-1 and KO-2 lines harbor only insertion alleles, whereas the pooled F₁ from each cross contain both alleles. Total ascorbate was determined in 2-week-old plants from each genotype (WT, *vtc4-1*, KO-1, KO-2, F₁ (*vtc4-1* × KO-1), and F₁ (*vtc4-1* × KO-2)). As seen in Fig. 7, A and C, the insertion lines do not genetically complement the ascorbate deficiency in *vtc4-1*, the F₁s containing an insertion allele and a *vtc4-1* allele are also ascorbate-deficient.

DISCUSSION

L-Gal-1-P phosphatase was recently purified and cloned by Laing *et al.* (23). However, they did not carry out a functional analysis, so the predicted role of this enzyme in ascorbate synthesis was not tested. Our results with the ascorbate-deficient *A. thaliana* mutant, *vtc4-1*, provide evidence that this enzyme is required for maximal ascorbate accumulation. First, *VTC4* maps to the predicted L-Gal-1-P phosphatase gene (At3g02870), which has a point mutation predicted to alter an active site domain in the resultant enzyme. Second, *vtc4-1* leaves have lower L-Gal-1-P phosphatase activity than WT. Third, an independent line with a T-DNA insertion in At3g02870 has low ascorbate, decreased L-Gal-1-P phosphatase activity, and is allelic to the *vtc4-1* allele. Finally, *in vivo* labeling experiments with [³H]Man showed that *vtc4-1* has perturbed L-Gal metabolism, as labeled L-galactosyl residues accumulated in polysaccharides in *vtc4-1*. Because GDP-L-Gal is the most likely source of these L-galactosyl residues, this observation suggests that the muta-

Ascorbate Synthesis in Plants via L-Gal-1-P Phosphatase

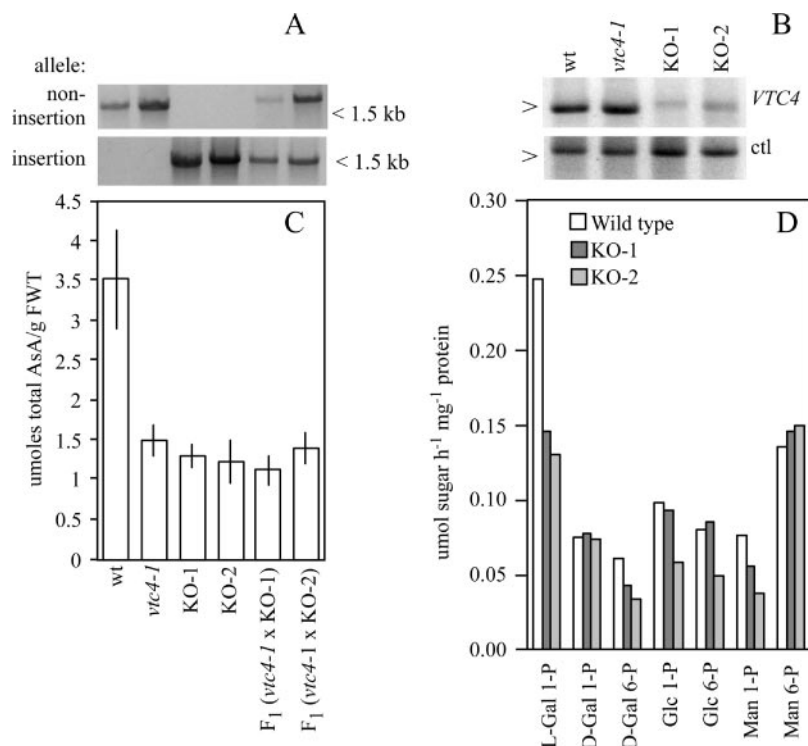


FIGURE 7. A T-DNA insertion mutant in At3g02870 is ascorbate-deficient and allelic to VTC4-1, and the insertion allele and the *vtc4-1* allele represent different alleles of the same gene. *A*, the genotypes of WT, *vtc4-1*, KO-1, KO-2, and pooled F₁ progeny from a cross between *vtc4-1* and KO-1 and a cross between *vtc4-1* and KO-2 were confirmed by PCR amplification of total DNA from each genotype. *Noninsertion allele* indicates the amplification product obtained from amplification of total DNA from each genotype with the VTC4B F/R gene-specific primers. *Insertion allele* indicates amplification product obtained from amplification of the above-mentioned DNAs with the LB1 SAIL line insert-specific internal primer and the opposing gene-specific primer VTC4B-R. The < indicates the position of the 1.5-kb size standard relative to the visualized PCR products. *B*, homozygous SAIL_843_G10 insertion lines KO-1 and KO-2 produce no VTC4 transcript as detected by RT-PCR. Total RNA was isolated from pooled WT, *vtc4-1*, KO-1, and KO-2 leaf tissue, and 1 μg from each genotype was reverse-transcribed into cDNAs using the VTC4RT-R and ferredoxin-nitrite reductase R (control) primers. The same volume of cDNA from each RT reaction was used in two separate parallel PCRs for each genotype with the addition of the VTC4RT-F and ferredoxin-nitrite reductase F primers. Amplification products were electrophoresed on a 3% agarose gel along with a 100-bp DNA ladder (Fermentas, Burlington, Ontario, Canada). Amplification products were visualized by ethidium bromide staining. *VTC4* indicates the RT-PCR products obtained with the VTC4RT-F/R primers; the *ctl* indicates the RT-PCR products obtained with the ferredoxin-nitrate reductase F/R primers. The > indicates the position of the 400-bp size standard relative to the visualized RT-PCR products. *C*, total ascorbic acid was assayed in pooled 3-week-old expanded leaves from each of the genotypes. The average ascorbate expressed as μmol/g fresh weight (FWT) is shown for each genotype (*n* = 3, assays from replicate extracts). Error bars for the S.D. are shown. *D*, comparison of phosphatase activity toward various sugar phosphates by WT, KO-1, and KO-2 extracts. Leaf extracts from plants just prior to flowering were fractionated by ammonium sulfate precipitation (45–60% saturation). The desalted sample was incubated with various sugar phosphates. Released sugars were measured by LC-pulsed amperometric detection.

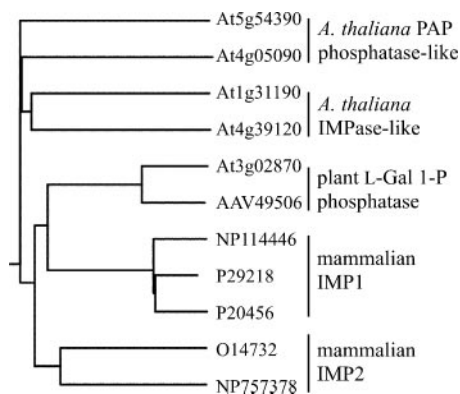


FIGURE 8. Phylogenetic relationship between the *Arabidopsis* polypeptides annotated as putative IMPases and known mammalian IMPases. Phylip phylogenetic inference software was used to determine this relationship. Note that the plant L-Gal-1-phosphate phosphatases (including VTC4, At3g02870) align much more closely with the mammalian IMPases than do the other *Arabidopsis* IMPase-like polypeptides or the PAP phosphatase-like polypeptides.

tion increases its availability as a substrate for glycosyltransferases. A possible explanation for this is that L-Gal-1-P inhibits the enzyme that converts GDP-L-Gal to L-Gal-1-P. Alternatively, the accumulating L-Gal-1-P could be converted to GDP-L-Gal by a pyrophosphorylase. Additional evidence for feedback control of the pathway comes from analysis of *A. thaliana* plants with antisense suppression of L-Gal dehy-

drogenase. Not only does L-Gal accumulate as predicted (18), but gas chromatography-mass spectrometry analysis shows that Man (including Man-1-P and GDP-Man) also accumulates,⁶ suggesting that accumulation of L-Gal feeds back to the GDP-Man-3,5-epimerase step (Fig. 1). Finally, in the L-Fuc-deficient *Arabidopsis* mutant *mur1* (defective in GDP-D-Man-4,6-dehydratase; see Ref. 42), L-Gal replaces L-Fuc in the cell wall xyloglucan (43) and rhamnogalacturonan II, a borate-binding pectin that is required for plant growth (44). As mammalian fucosyltransferase is able to utilize GDP-L-Gal as a substrate (45), it has been hypothesized that fucosyltransferase in *mur1* is using GDP-L-Gal in the absence of GDP-L-Fuc (46). This implies that excess GDP-Man in *mur1* is converted to GDP-L-Gal, which is then shunted into the cell wall and not into ascorbic acid, most likely due to the above-mentioned feedback control. As well as being required for ascorbate synthesis, an L-Gal residue occurs in side chain A of rhamnogalacturonan II (44). Therefore, further investigation of how GDP-L-Gal is partitioned between rhamnogalacturonan II and ascorbate synthesis would be fruitful given that reduced ascorbate synthesis increases L-Gal accumulation in polysaccharides in *vtc4-1*.

The *Arabidopsis* L-Gal-1-P phosphatase (At3g02870/VTC4) is annotated by the *Arabidopsis* genome data bases as a putative inositol/*myo*-inositol monophosphatase (IMPase; TAIR, TIGR, and MIPS). Four

⁶ S. Gatzek, N. Smirnov, and O. Fiehn, unpublished data.

additional unlinked genes in the *Arabidopsis* genome have also been annotated as encoding putative IMPases (At1g31190, At4g05090, At4g39120, and At5g54390). As detailed above, it is clear that At3g02870/*VTC4* encodes an enzyme with high specificity for L-Gal-1-P. Previously it was shown that this enzyme is ~12 times more active against L-Gal-1-P than against *myo*-inositol-1-P (23). By using the Phylip phylogenetic inference software, the relationship between the predicted polypeptides encoded by these five IMPase-like genes and to mammalian IMPases was determined and is shown in Fig. 8. As expected, At3g02870 closely aligns with the *A. deliciosa* L-Gal-1-P phosphatase, and in fact, these two polypeptides share 79% amino acid identity. All five *Arabidopsis* gene products reside in the superfamily of metal-dependent phosphatases (HomoloGene cd01636). However, At5g54390 and At4g05090 both encode polypeptides with a predicted 3'-phosphoadenosine 5'-phosphate (PAP) phosphatase domain that places them into a different subgroup (cd1517) than that of the plant L-Gal-1-Pases and the IMPases that utilize mainly inositol monophosphate as a substrate (HomoloGene). Indeed, At5g54390 was previously identified as a *HAL2*-like gene (*AtAHL*) that encodes an enzyme shown experimentally to have sodium-sensitive PAP phosphatase activity (47). Two additional PAP phosphatase genes are present in the *Arabidopsis* genome (*AtSAL1* and *AtSAL2* (47)) but are annotated as encoding putative inositol polyphosphate 1-phosphatases (or 3'(2'),5'-bispophosphate nucleotidases). Therefore, At4g05090 may be a fifth gene in a PAP phosphatase gene family. The two other IMPase-like genes (At1g31190 and At4g39120) encode polypeptides that are more closely related to each other than to the L-Gal-1-P phosphatases or to the PAP phosphatases, yet the predicted polypeptides both contain the conserved IMPase domain and may therefore have high specificity toward *myo*-inositol. Although it is true that these two polypeptides share only 29–35% amino acid identity with three tomato enzymes shown to have IMPase activity, the activity of the tomato enzymes was only tested against inositol-1-P (48). Indeed, the tomato enzymes are much more closely aligned with the L-Gal-1-P phosphatases (~72 to 76% identity) and, as also noted by Laing *et al.* (23), may therefore actually have much greater phosphatase activity against L-Gal-1-P than inositol-1-P. It is interesting to note that the mammalian IMPase 1 enzymes are more closely related to *Arabidopsis* L-Gal-1-P phosphatases than to the putative PAP phosphatases or the putative IMPases.

The combined genetic and biochemical data presented here provide definitive *in planta* evidence for the role of L-Gal-1-P phosphatase in plant ascorbic acid biosynthesis. Although the radiolabeling experiments and the rapid conversion of L-Gal to ascorbate by plants suggest L-Gal-1-P is the substrate, it is also possible that the enzyme could work on L-Gul-1-P, thereby leading to ascorbate synthesis via L-gulonolactone (Fig. 1) (21). Importantly, the KO mutant still contains appreciable ascorbate, even though At3g02870 is not expressed. This suggests that other enzymes, such as the other IMPase homologues, can hydrolyze L-Gal-1-P and/or L-Gul-1-P *in vivo* or that the remaining ascorbate is synthesized via other pathways. Recently, evidence from transgenic manipulation has suggested pathways for ascorbate synthesis via D-galacturonic acid (49) and glucuronic acid (50). Interestingly, the recombinant enzyme hydrolyzes *myo*-inositol-1-P at 7% of the rate of L-Gal-1-P (23), suggesting it may have a role in ascorbate synthesis via glucuronate. At3g02870/*VTC4* could therefore contribute to both the L-Gal and the *myo*-inositol pathways. Both the KO mutant and *vtc4-1* have a similar decrease in L-Gal-1-P phosphatase activity. The sequence conservation of the substrate and Mg²⁺-binding residues shown by comparison with human inositol monophosphatase, and which includes the site of the P92L mutation in *VTC4-1*, suggests that the

enzyme would have significantly reduced activity. This observation would explain the similarity in enzyme activity between *vtc4-1* and the KO mutant. All the genes involved in synthesis of ascorbate from D-Man-1-P, with the exception of the step that converts GDP-L-Gal to L-Gal-1-P, have now been identified (Fig. 1). We are currently in the process of the functional characterization of the *VTC2* and *VTC3* genes. We predict that the identification of all the enzymes of the proposed D-Man/L-Gal pathway for ascorbate biosynthesis in plants (15) will soon be completed. This will provide a strong basis for understanding the control of ascorbate accumulation in plants and for investigating the contribution of pathways involving L-Gul (21) and uronic acid intermediates (49, 51).

Acknowledgments—We thank both Jamie Brenchley and Brian Conlin for their contributions to the mapping of *VTC4*. We are indebted to Prof. J. Thiem (University of Hamburg, Germany) for the gift of L-Gal-1-P.

REFERENCES

- King, C. G., and Waugh, W. A. (1932) *Science* **75**, 357–358
- Svirbely, J. L., and Szent-Gyorgi, A. (1932) *Nature* **129**, 576
- de Tullio, M. (2004) in *Vitamin C: Function and Biochemistry in Animals and Plants* (Asard, H., May, J. M., and Smirnov, N., eds) pp. 159–171, Bios Scientific Publishers, Oxford
- Buettner, G. R., and Schafer, F. Q. (2004) in *Vitamin C: Function and Biochemistry in Animals and Plants* (Asard, H., May, J. M., and Smirnov, N., eds) pp. 173–188, Bios Scientific Publishers, Oxford
- May, J. M., and Asard, H. (2004) in *Vitamin C: Function and Biochemistry in Animals and Plants* (Asard, H., May, J. M., and Smirnov, N., eds) pp. 139–157, Bios Scientific Publishers, Oxford
- Barth, C., Moeder, W., Klessig, D. F., and Conklin, P. L. (2004) *Plant Physiol.* **134**, 1784–1792
- Conklin, P. L., Williams, E. H., and Last, R. L. (1996) *Proc. Natl. Acad. Sci. U. S. A.* **93**, 9970–9974
- Conklin, P. L., and Barth, C. (2004) *Plant Cell Environ.* **27**, 959–970
- Filkowski, J., Kovalchuk, O., and Kovalchuk, I. (2004) *Plant J.* **38**, 60–69
- Pastori, G. M., Kiddle, G., Antoni, J., Bernard, S., Veljovic-Jovanovic, S., Verrier, P. J., Noctor, G., and Foyer, C. H. (2003) *Plant Cell* **15**, 939–951
- Conklin, P. L., Saracco, S. A., Norris, S. R., and Last, R. L. (2000) *Genetics* **154**, 847–856
- Muller-Moule, P., Conklin, P. L., and Niyogi, K. K. (2002) *Plant Physiol.* **128**, 970–977
- Muller-Moule, P., Havaux, M., and Niyogi, K. K. (2003) *Plant Physiol.* **133**, 748–760
- Jander, G., Norris, S. R., Rounsley, S. D., Bush, D. F., Levin, I. M., and Last, R. L. (2002) *Plant Physiol.* **129**, 440–450
- Wheeler, G. L., Jones, M. A., and Smirnov, N. (1998) *Nature* **393**, 365–369
- Smirnov, N., Conklin, P. L., and Loewus, F. A. (2001) *Annu. Rev. Plant Physiol. Plant Mol. Biol.* **52**, 437–467
- Conklin, P. L., Norris, S. R., Wheeler, G. L., Williams, E. H., Smirnov, N., and Last, R. L. (1999) *Proc. Natl. Acad. Sci. U. S. A.* **96**, 4198–4203
- Gatzek, S., Wheeler, G. L., and Smirnov, N. (2002) *Plant J.* **30**, 541–553
- Wolucka, B. A., Persiau, G., Van Doorselaere, J., Davey, M. W., Demol, H., Vandekerckhove, J., Van Montagu, M., Zabeau, M., and Boerjan, W. (2001) *Proc. Natl. Acad. Sci. U. S. A.* **98**, 14843–14848
- Ostergaard, J., Persiau, G., Davey, M. W., Bauw, G., and Van Montagu, M. (1997) *J. Biol. Chem.* **272**, 30009–30016
- Wolucka, B. A., and Van Montagu, M. (2003) *J. Biol. Chem.* **278**, 47483–47490
- Tabata, K., Oba, K., Suzuki, K., and Esaka, M. (2001) *Plant J.* **27**, 139–148
- Laing, W. A., Bulley, S., Wright, M., Cooney, J., Jensen, D., Barraclough, D., and MacRae, E. (2004) *Proc. Natl. Acad. Sci. U. S. A.* **101**, 16976–16981
- Conklin, P. L., Pallanca, J. E., Last, R. L., and Smirnov, N. (1997) *Plant Physiol.* **115**, 1277–1285
- Lukowitz, W., Nickle, T. C., Meinke, D. W., Last, R. L., Conklin, P. L., and Somerville, C. R. (2001) *Proc. Natl. Acad. Sci. U. S. A.* **98**, 2262–2267
- Sessions, A., Burke, E., Presting, G., Aux, G., McElver, J., Patton, D., Dietrich, B., Ho, P., Bacwaden, J., Ko, C., Clarke, J. D., Cotton, D., Bullis, D., Snell, J., Miguel, T., Hutchison, D., Kimmerly, B., Mitzel, T., Katagiri, F., Glazebrook, J., Law, M., and Goff, S. A. (2002) *Plant Cell* **14**, 2985–2994
- Pallanca, J. E., and Smirnov, N. (2000) *J. Exp. Bot.* **51**, 669–674
- Fry, S. C. (1988) *The Growing Plant Cell Wall: Chemical and Metabolic Analysis*, Longman Scientific & Technical, Harlow, UK
- Ghebregzabher, M., Rufini, S., Monaldi, B., and Lato, M. (1976) *J. Chromatogr.* **127**,

Ascorbate Synthesis in Plants via L-Gal-1-P Phosphatase

- 133–162
30. Rhee, S. Y., Beavis, W., Berardini, T. Z., Chen, G. H., Dixon, D., Doyle, A., Garcia-Hernandez, M., Huala, E., Lander, G., Montoya, M., Miller, N., Mueller, L. A., Mundodi, S., Reiser, L., Tacklind, J., Weems, D. C., Wu, Y. H., Xu, L., Yoo, D., Yoon, J., and Zhang, P. F. (2003) *Nucleic Acids Res.* **31**, 224–228
31. Zhang, Y., Liang, J. Y., and Lipscomb, W. N. (1993) *Biochem. Biophys. Res. Commun.* **190**, 1080–1083
32. Schwede, T., Kopp, J., Guex, N., and Peitsch, M. C. (2003) *Nucleic Acids Res.* **31**, 3381–3385
33. Gill, R., Mohammed, F., Badyal, R., Coates, L., Erskine, P., Thompson, D., Cooper, J., Gore, M., and Wood, S. (2005) *Acta Crystallogr. Sect. D Biol. Crystallogr.* **61**, 545–555
34. Frossard, E., Bucher, M., Machler, F., Mozafar, A., and Hurrell, R. (2000) *J. Sci. Food Agric.* **80**, 861–879
35. Ganzhorn, A. J., and Rondeau, J. M. (1997) *Protein Eng.* **10**, 61
36. Bone, R., Frank, L., Springer, J. P., Pollack, S. J., Osborne, S., Atack, J. R., Knowles, M. R., Mcallister, G., Ragan, C. I., Broughton, H. B., Baker, R., and Fletcher, S. R. (1994) *Biochemistry* **33**, 9460–9467
37. Chan, A. W. E., Hutchinson, E. G., Harris, D., and Thornton, J. M. (1993) *Protein Sci.* **2**, 1574–1590
38. Baydoun, E. A. H., and Fry, S. C. (1988) *J. Plant Physiol.* **132**, 484–490
39. Bonin, C. P., and Reiter, W. D. (2000) *Plant J.* **21**, 445–454
40. Roberts, R. M. (1971) *Arch. Biochem. Biophys.* **145**, 685–692
41. Seifert, G. J. (2004) *Curr. Opin. Plant Biol.* **7**, 277–284
42. Bonin, C. P., Potter, I., Vanzin, G. F., and Reiter, W. D. (1997) *Proc. Natl. Acad. Sci. U. S. A.* **94**, 2085–2090
43. Zablackis, E., York, W. S., Pauly, M., Hantus, S., Reiter, W. D., Chapple, C. C. S., Albersheim, P., and Darvill, A. (1996) *Science* **272**, 1808–1810
44. Reuhs, B. L., Glenn, J., Stephens, S. B., Kim, J. S., Christie, D. B., Glushka, J. G., Zablackis, E., Albersheim, P., Darvill, A. G., and O'Neill, M. A. (2004) *Planta* **219**, 147–157
45. Duffels, A., Green, L. G., Lenz, R., Ley, S. V., Vincent, S. P., and Wong, C. H. (2000) *Bioorg. Med. Chem.* **8**, 2519–2525
46. O'Neill, M. A., Eberhard, S., Albersheim, P., and Darvill, A. G. (2001) *Science* **294**, 846–849
47. Gil-Mascarell, R., Lopez-Coronado, J. M., Belles, J. M., Serrano, R., and Rodriguez, P. L. (1999) *Plant J.* **17**, 373–383
48. Gillaspay, G. E., Keddie, J. S., Oda, K., and Gruissem, W. (1995) *Plant Cell* **7**, 2175–2185
49. Agius, F., Gonzalez-Lamothe, R., Caballero, J. L., Munoz-Blanco, J., Botella, M. A., and Valpuesta, V. (2003) *Nat. Biotechnol.* **21**, 177–181
50. Lorence, A., Chevone, B. I., Mendes, P., and Nessler, C. L. (2004) *Plant Physiol.* **134**, 1200–1205
51. Radzio, J. A., Lorence, A., Chevone, B. I., and Nessler, C. L. (2003) *Plant Mol. Biol.* **53**, 837–844
52. Millar, A. H., Mittova, V., Kiddle, G., Heazlewood, J. L., Bartoli, C. G., Theodoulou, F. L., and Foyer, C. H. (2003) *Plant Physiol.* **133**, 443–447
53. Davey, M. W., Gilot, C., Persiau, G., Ostergaard, J., Han, Y., Bauw, G. C., and Van Montagu, M. C. (1999) *Plant Physiol.* **121**, 535–543